Orbital Ordering in $La_{0.5}Sr_{1.5}MnO_4$ Studied by Soft X-Ray Linear Dichroism

D. J. Huang,[1,2] W. B. Wu,[2,1] G. Y. Guo,[3,1] H.-J. Lin,[1] T. Y. Hou,[1] C. F. Chang,[1] C. T. Chen,[1,3] A. Fujimori,[4] T. Kimura,[5,*] H. B. Huang,[6] A. Tanaka,[6] and T. Jo[6]

[1]*National Synchrotron Radiation Research Center, Hsinchu 30077, Taiwan*
[2]*Department of Electrophysics, National Chiao-Tung University, Hsinchu 300, Taiwan*
[3]*Department of Physics, National Taiwan University, Taipei 106, Taiwan*
[4]*Department of Physics and Department of Complexity Science and Engineering, University of Tokyo, Tokyo 113-0033, Japan*
[5]*Department of Applied Physics, University of Tokyo, Tokyo 113-8656, Japan*
[6]*Department of Quantum Matters, ADSM, Hiroshima University, Higashi-Hiroshima 739-8530, Japan*

(Received 8 May 2003; revised manuscript received 17 November 2003; published 26 February 2004)

We found that the conventional model of orbital-ordering of $3x^2 - r^2/3y^2 - r^2$ type in the e_g states of $La_{0.5}Sr_{1.5}MnO_4$ is incompatible with measurements of linear dichroism in the Mn $2p$-edge x-ray absorption, whereas these e_g states exhibit predominantly cross-type orbital ordering of $x^2 - z^2/y^2 - z^2$. LDA + U band-structure calculations reveal that such a cross-type orbital-ordering results from a combined effect of antiferromagnetic structure, Jahn-Teller distortion, and on-site Coulomb interactions.

DOI: 10.1103/PhysRevLett.92.087202 PACS numbers: 75.47.Lx, 71.28.+d, 75.30.Mb, 78.70.Dm

Orbital ordering, which manifests itself in the spatial distribution of the outermost valence electrons, is an important topic in current research of transition-metal oxides, as the magnetic and transport properties are closely related to the orbital and charge degrees of freedom [1]. In particular, charge-orbital ordering of half-doped manganites has attracted much attention [2–8]. The mechanism of charge-orbital ordering is being hotly debated [9–15]. To observe orbital ordering directly is a difficult task. Experimental results of resonant x-ray scattering (RXS) at the Mn K edge in $La_{0.5}Sr_{1.5}MnO_4$ and $LaMnO_3$ show removal of degeneracy between $4p_x$ and $4p_y$; these observations have been argued to be direct evidence of orbital ordering [16,17]. However, the origin of RXS at Mn K edge is controversial. Orbital ordering in transition-metal oxides is typically accompanied by Jahn-Teller lattice distortion. Calculations based on a local-density approximation including on-site Coulomb interactions (LDA + U) [18,19] and multiple scattering theory [20] indicate that RXS measurements pertain mainly to Jahn-Teller distortion, instead of directly observing $3d$ orbital ordering. Multiplet calculations have shown that one can use linear dichroism (LD) in soft x-ray absorption spectroscopy (XAS) to identify the orbital character of $3d$ states in orbital-ordered manganites [21].

Half-doped manganites such as $La_{0.5}Sr_{1.5}MnO_4$ exhibit CE-type [3] antiferromagnetic (AFM) ordering and charge-orbital ordering [16,22,23]. They have a zigzag magnetic structure in which the magnetic moments of Mn on the chain form a ferromagnetic coupling, but AFM coupling between the zigzag chains. Below the charge-ordering (CO) temperature $T_{CO} = 217$ K, the valence of $La_{0.5}Sr_{1.5}MnO_4$ orders in an alternating pattern with two distinct sites identified as Mn^{3+} and Mn^{4+} [22,23]. The e_g electrons on the nominal Mn^{3+} sites of $La_{0.5}Sr_{1.5}MnO_4$ are believed to exhibit an orbital ordering of $3x^2 - r^2/3y^2 - r^2$, in which occupied $d_{3x^2-r^2}$ and $d_{3y^2-r^2}$ orbitals are alternately arranged at two sublattices in the ab plane [7]. However, $d_{3x^2-r^2}$ and $d_{x^2-z^2}$ ($d_{3y^2-r^2}$ and $d_{y^2-z^2}$) orbitals might be mixed, because orbitals of these two types have the same spatial symmetry with respect to the MnO_2 plane. To clarify the nature of orbital ordering in $La_{0.5}Sr_{1.5}MnO_4$ is essential to reveal the origin of orbital-ordering in half-doped manganites.

In this Letter, we present measurements of LD in Mn $2p$-edge XAS of $La_{1-x}Sr_{1+x}MnO_4$. The LD measurements are compared with multiplet calculations to unravel the orbital character of e_g electrons in $La_{0.5}Sr_{1.5}MnO_4$. We performed also LDA + U calculations to study the orbital ordering of this compound.

Single-crystalline samples of $La_{1-x}Sr_{1+x}MnO_4$ were grown by the floating zone method [22]. Measurements of x-ray diffraction at room temperature show that our samples are of single phase. The major crystallographic difference between crystals with different x's is the c-axis length; this decreases significantly from 13.04 Å for $x = 0$ to 12.43 Å for $x = 0.5$, whereas the a-axis length shows only a weak x dependence (3.81 Å for $x = 0$ and 3.86 Å for $x = 0.5$). This difference of the c-axis length is attributed to a significantly decreased out-of-plane Mn-O bond length with increasing Sr content.

XAS measurements on $La_{1-x}Sr_{1+x}MnO_4$ single crystals at various temperatures were performed at the Dragon beamline of the National Synchrotron Radiation Research Center in Taiwan. We recorded XAS spectra by collecting the sample drain current. Crystals were freshly cleaved in an ultrahigh vacuum at 90 K; the incident angle was 60° from the sample surface normal, and the photon energy resolution was 0.2 eV. We rotated the sample about the direction of incident photons to obtain LD spectra from which experimental artifacts related to the difference in the optical path and to the probing area

have been eliminated. All measured XAS spectra referred to the **E** vector parallel to the c axis are shown with a correction for the geometry effect [24,25].

Multiplet calculations have shown that one can use LD in L-edge XAS to characterize the $3d$ orbital character [21]. LD in XAS is defined as the difference between XAS spectra taken with the **E** vector of photons perpendicular and parallel to the crystal c axis. To verify experimentally such a capability of LD, we measured the LD in Mn $L_{2,3}$-edge XAS of $LaSrMnO_4$, which is expected to exhibit $3z^2 - r^2$ "ferro-orbital" ordering. Figure 1(a) shows our measurements of polarization-dependent XAS and LD on $LaSrMnO_4$. Most features in the measured LD at Mn L edge are reproduced by multiplet calculations for Mn^{3+} ions with occupied $d_{3z^2-r^2}$ orbitals, as shown in Fig. 1(b) [21,26], revealing that LD in L-edge XAS is an effective means to examine the orbital character of $3d$ electronic states in an orbital-ordered compound.

We measured also the LD in XAS on $La_{1-x}Sr_{1+x}MnO_4$ with varied doping to clarify further the origin of the LD signal, as shown in Fig. 2(a). Because the Jahn-Teller effect on the Mn^{4+} ions is insignificant [14,15], the contribution of $3d$ orbitals of these ions to LD is much smaller than that of Mn^{3+} ions. With increasing doping, the proportion of Mn^{3+} ions decreases; the LD magnitude of doped $La_{1-x}Sr_{1+x}MnO_4$ diminishes. Note that the magnitude of LD decreases more rapidly than that from a simple picture of Mn^{3+}-Mn^{4+} dilution. In particular, the LD magnitude of $La_{0.5}Sr_{1.5}MnO_4$ is $\sim 1/4$ that observed for $LaSrMnO_4$; its sign at the L_2 edge is the same as that of $LaSrMnO_4$. To identify the orbital character of the occupied e_g states, by using a model of MnO_6 cluster based on configuration interaction [27], we calculated LD spectra of Mn^{3+} with $d_{x^2-z^2}/d_{y^2-z^2}$ and $d_{3x^2-r^2}/d_{3y^2-r^2}$ orbitals occupied, as shown in Fig. 2(b) [28]. Overall the calculated LD of occupied in-plane orbitals such as $d_{3x^2-r^2}$ and $d_{3y^2-r^2}$ is with sign reversed to that of out-of-plane orbitals such as $d_{3z^2-r^2}$, $d_{x^2-z^2}$, and $d_{y^2-z^2}$. Surprisingly the conventional orbital-ordering model of $3x^2 - r^2/3y^2 - r^2$ type is incompatible with LD measurements. The calculated LD of $3x^2 - r^2/3y^2 - r^2$-type orbital ordering is with sign reversed to that of measured LD from $La_{0.5}Sr_{1.5}MnO_4$. One might suspect this inconsistency could result from anisotropic e_g charge distribution on the Mn^{4+} sites. If so, only e_g charge with $d_{3z^2-r^2}$ or $d_{x^2-z^2}/d_{y^2-z^2}$ polarization transferred from Mn^{3+} to Mn^{4+} could give rise to a LD similar to the measurement. However, even in the most unfavorable case, that is, even if the transferred e_g charge on the Mn^{4+} site were maximum (leading to equal charges on both Mn sites) and fully $(3z^2 - r^2)$ polarized, only half of the observed LD could be accounted for. As shown later (see the lower panel of Fig. 3), such transferred e_g charges, indeed, have a small in-plane polarization. This anisotropy gives opposite contributions to LD with respect to the measurement; the inconsistency cannot be reconciled even if the anisotropic charge distribution of Mn^{4+} is taken into account.

Furthermore, the line shape of the measured LD spectrum for $x = 0.5$ is similar to those from calculations for

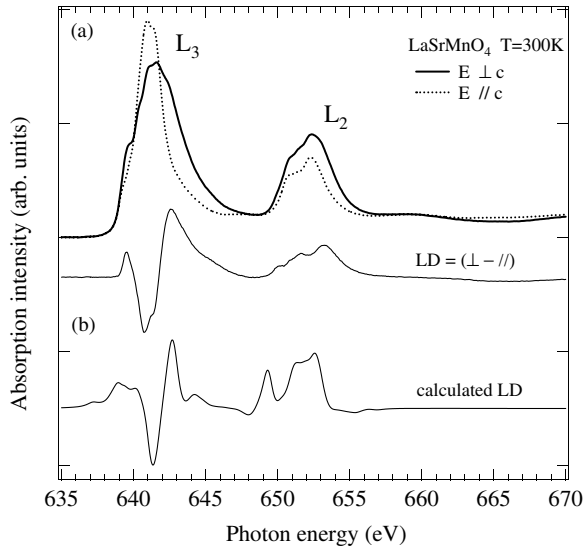

FIG. 1. (a) LD and polarization-dependent XAS taken with $\mathbf{E} \perp c$ (solid line) and $\mathbf{E} \parallel c$ (broken line) of $LaSrMnO_4$. (b) Calculated LD spectrum of Mn^{3+} ions with occupied $d_{3z^2-r^2}$ orbitals. The calculated LD is plotted on the same scale as the measured one.

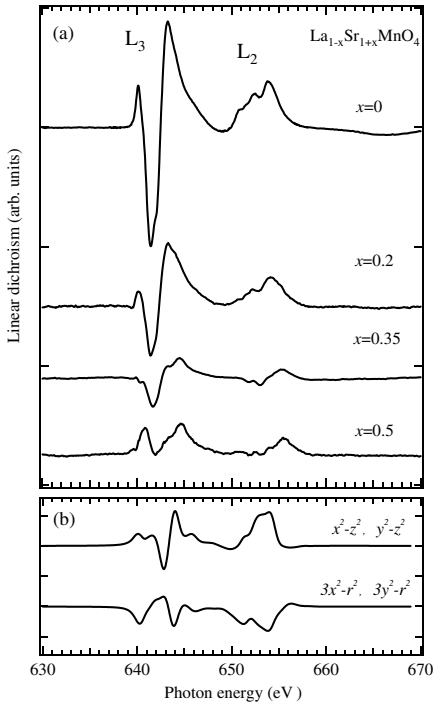

FIG. 2. (a) LD in Mn $L_{2,3}$-edge XAS of $La_{1-x}Sr_{1+x}MnO_4$ with varied doping. Linear-dichroism spectra were derived from XAS normalized to the same peak intensity at Mn L_3 edge and measured at 300 K for $x \leq 0.35$ and 150 K for $x = 0.5$. (b) Calculated LD spectra of Mn^{3+} ions with $d_{x^2-z^2}/d_{y^2-z^2}$ and $d_{3x^2-r^2}/d_{3y^2-r^2}$ orbitals occupied.

Mn^{3+} with occupied $d_{3z^2-r^2}$ or $d_{x^2-z^2}/d_{y^2-z^2}$ orbitals, implying that $La_{0.5}Sr_{1.5}MnO_4$ has an orbital polarization of strong z character, e.g., $d_{3z^2-r^2}$ or $d_{x^2-z^2}/d_{y^2-z^2}$. If $La_{0.5}Sr_{1.5}MnO_4$ exhibited $3z^2 - r^2$ orbital ordering, all Mn^{3+} sites, i.e., half of all Mn atoms, would contribute to LD and its magnitude at Mn L_2 edge would be half of that observed in $LaSrMnO_4$, in contrast to the measurements. If $La_{0.5}Sr_{1.5}MnO_4$ exhibits $x^2 - z^2/y^2 - z^2$ orbital ordering, by choosing LD as the difference in XAS spectra taken with the **E** vector parallel to x and z axes, we observe essentially linear dichroism resulting only from the sublattice with occupied $d_{y^2-z^2}$. In other words, only half of the Mn^{3+} sites contribute to LD; one quarter of the Mn atoms contribute to LD, consistent with the measurements. Our LD measurements thus suggest that orbital ordering of the e_g states on the Mn site in $La_{0.5}Sr_{1.5}MnO_4$ is dominated by $x^2 - z^2/y^2 - z^2$ type.

To further study orbital ordering in $La_{0.5}Sr_{1.5}MnO_4$, we performed LDA + U calculations using the full-potential linearized augmented-plane-wave method on $La_{0.5}Sr_{1.5}MnO_4$ in CE-type AFM structure with U and J equal to 8 and 0.88 eV for Mn 3d electrons, respectively [18]. Details of the calculations will be described elsewhere [29]. Mahadevan *et al.* [14] found that the breathing-type Jahn-Teller distortion of $La_{0.5}Sr_{1.5}MnO_4$ suggested by Sternlieb *et al.* [23] is not energetically favorable, and proposed a shear-type Jahn-Teller distortion in which the Mn-O length is elongated alternately along the x and y directions. Measurements of x-ray scattering also indicate a shear-type distortion on Mn-O octahedra [30], rather than a breathing-type distortion. Consistent with previous band-structure calculations [14], our LDA + U calculations show also that $La_{0.5}Sr_{1.5}MnO_4$ without Jahn-Teller distortion is unstable against a shear-type Jahn-Teller distortion. With a shear-type Jahn-Teller distortion of 0.08-Å in-plane O displacement [31], LDA + U calculations give rise to an orbital ordering dominated by $x^2 - z^2/y^2 - z^2$ on the Mn^{3+} sites of $La_{0.5}Sr_{1.5}MnO_4$, as shown in Fig. 3, which displays charge-density contours corresponding to the e_g dominated valence bands. Interestingly, we found also that $La_{0.5}Sr_{1.5}MnO_4$ would exhibit $3x^2 - r^2/3y^2 - r^2$ orbital ordering if the on-site Coulomb interactions were not explicitly included, in agreement with previous LDA calculations [14]. Our results suggest that charge and orbital ordering can be well described if the on-site Coulomb interactions of 3d electrons are properly taken into account, as in the LDA + U or Hartree-Fock calculations. Such a cross-type orbital ordering results from a combined effect of AFM structure, Jahn-Teller distortion, and the on-site Coulomb interactions of 3d electrons.

The existence of orbital ordering of cross-type $x^2 - z^2/y^2 - z^2$ can be understood within the framework of crystal field effect with lattice distortion taken into account. On the Mn^{3+} sites of a cubic perovskite, e_g orbitals of $3y^2 - r^2$ ($3x^2 - r^2$) symmetry are preferentially occupied if the Mn-O length is elongated along the y (x) direction; $y^2 - z^2$ ($x^2 - z^2$) orbitals are occupied if the Mn-O length is contracted along the x (y) direction, as shown in Fig. 4. For example, in CE-type charge-orbital-ordered half-doped manganites of cubic perovskite such as $La_{0.5}Ca_{0.5}MnO_3$, the Mn^{3+} site exhibits a large Jahn-Teller distortion, in which the Mn-O length is elongated alternately along the x and y directions (two long bonds of 2.06 Å along the zigzag chain and four short bonds of 1.92 Å) [32], producing $3x^2 - r^2/3y^2 - r^2$ orbital ordering. As for $La_{0.5}Sr_{1.5}MnO_4$, the shear-type distortion leads effectively to alternate contractions along the x and y directions in $La_{0.5}Sr_{1.5}MnO_4$, because the longer in-plane Mn-O length (2.00 Å) is close to the out-of-plane Mn-O length (1.98 Å), while the shorter

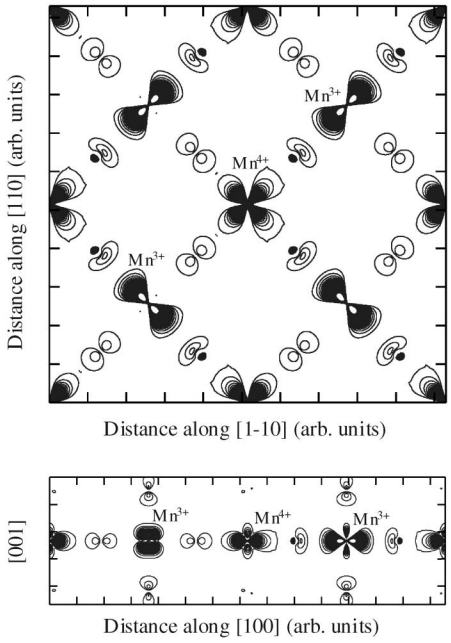

FIG. 3. Charge-density contours corresponding to the e_g valence bands of $La_{0.5}Sr_{1.5}MnO_4$. Upper panel: Charge-density contours in the ab plane. Lower panel: Charge-density contours in the ac plane along the [100] direction.

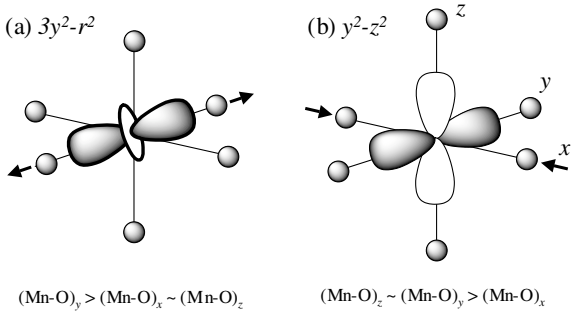

FIG. 4. View of $d_{3y^2-r^2}$ and $d_{x^2-z^2}$ orbitals on the Mn^{3+} sites with different Jahn-Teller distortions. (a),(b) The Mn-O length elongated along the y direction and contracted along the x direction, respectively. Filled circles denote O atoms in which 2p orbitals are omitted for clarity.

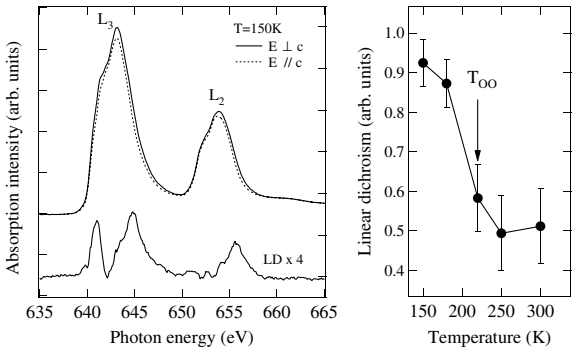

FIG. 5. Left panel: XAS and LD spectra of $La_{0.5}Sr_{1.5}MnO_4$ recorded at temperatures 150 K. Right panel: temperature dependence of relative LD in XAS measured at temperatures about T_{CO}. The solid line is for visual guidance. Error bars reflect uncertainties from different sets of data.

in-plane Mn-O length is 1.84 Å. Orbital ordering of $x^2 - z^2/y^2 - z^2$ is expected to be energetically more favorable than that of $3x^2 - r^2/3y^2 - r^2$. Note that small tetragonal distortions with $c/a = 0.98$ and $c/a = 1.04$ in strained thin films of $La_{0.5}Sr_{0.5}MnO_3$ can result in ferro-orbital ordering of $x^2 - y^2$ and $3z^2 - r^2$, respectively [33,34].

In addition, measurements of temperature-dependent LD of $La_{0.5}Sr_{1.5}MnO_4$ about T_{CO} provide us with further evidence that LD in XAS reflects the nature of orbital ordering. LD measurements with photon energy of 645 eV show that the LD decreases greatly as the temperature crosses T_{CO}, as shown in Fig. 5, indicating that orbital ordering of $La_{0.5}Sr_{1.5}MnO_4$ follows a similar temperature-dependent trend of charge ordering [23] and Jahn-Teller distortion [16]. To confirm this, more detailed temperature-dependent studies are necessary.

To conclude, we demonstrate that LD in Mn $2p$ XAS is a powerful method to test the validity of models for orbital ordering in transition-metal oxides. With LD measurements, we inferred that orbital ordering of the Mn e_g electrons in $La_{0.5}Sr_{1.5}MnO_4$ is dominated by $x^2 - z^2/y^2 - z^2$ type, as corroborated by our LDA + U calculations. Orbital ordering of Mn e_g electrons in $La_{0.5}Sr_{1.5}MnO_4$ results from a combined effect of antiferromagnetic structure, Jahn-Teller distortion, and on-site Coulomb interactions. In principle, one can directly observe both orbital ordering and Jahn-Teller ordering in manganites by using resonant x-ray scattering at Mn $L_{2,3}$ edges [35].

We thank Y. Tokura, T. Mizokawa, P. Mahadevan, and C. H. Chen for valuable discussions. We also thank L. H. Tjeng for loaning his XAS chamber. This work was supported in part by the National Science Council of Taiwan and by a Grant-in-Aid for Scientific Research in Priority Area "Novel Quantum Phenomena in Transition-Metal Oxides" from the Ministry of Education, Culture, Sports, Science and Technology of Japan.

*Present address: Los Alamos National Laboratory, MST-MISL, Mail Stop K774, Los Alamos, New Mexico 87545, USA.

[1] Y. Tokura and N. Nagaosa, Science **288**, 462 (2000).
[2] J. B. Goodenough, Phys. Rev. **100**, 564 (1955).
[3] E. O. Wollan and W. C. Koehler, Phys. Rev. **100**, 545 (1955).
[4] Y. Okimoto *et al.*, Phys. Rev. Lett. **75**, 109 (1995).
[5] P. Schiffer *et al.*, Phys. Rev. Lett. **75**, 3336 (1995).
[6] P. G. Radaelli *et al.*, Phys. Rev. B **55**, 3015 (1997).
[7] T. Mizokawa and A. Fujimori, Phys. Rev. B **56**, 493 (1997).
[8] S. Mori, C. H. Chen, and S.-W. Cheong, Nature (London) **392**, 473 (1998).
[9] T. Mutou and H. Kontani, Phys. Rev. Lett. **83**, 3685 (1999).
[10] D. Khomskii and J. van den Brink, Phys. Rev. Lett. **85**, 3329 (2000).
[11] T. Hotta *et al.*, Phys. Rev. Lett. **86**, 2478 (2001).
[12] T. Mutou and H. Kontani, Phys. Rev. Lett. **86**, 2479 (2001).
[13] J. van den Brink *et al.*, Phys. Rev. Lett. **83**, 5118 (1999).
[14] P. Mahadevan, K. Terakura, and D. D. Sarma, Phys. Rev. Lett. **87**, 066404 (2001).
[15] Z. Popovic and S. Satpathy, Phys. Rev. Lett. **88**, 197201 (2002).
[16] Y. Murakami *et al.*, Phys. Rev. Lett. **80**, 1932 (1998).
[17] Y. Murakami *et al.*, Phys. Rev. Lett. **81**, 582 (1998).
[18] I. S. Elfimov, V. I. Anisimov, and G. A. Sawatzky, Phys. Rev. Lett. **82**, 4264 (1999).
[19] P. Benedetti *et al.*, Phys. Rev. B **63**, 60408 (2001).
[20] M. Benfatto, Y. Joly, and C. R. Natoli, Phys. Rev. Lett. **83**, 636 (1999).
[21] H. B. Huang *et al.*, J. Phys. Soc. Jpn. **69**, 2399 (2000); H. B. Huang and T. Jo, *ibid.* **71**, 3094 (2001).
[22] Y. Moritomo *et al.*, Phys. Rev. B **51**, 3297 (1995).
[23] B. J. Sternlieb *et al.*, Phys. Rev. Lett. **76**, 2169 (1996).
[24] XAS intensity $I_{\|}$ for $\mathbf{E} \| c$ is deduced from $I_{\|} = \frac{4}{3}(I - \frac{1}{4}I_{\perp})$, in which $I_{\perp}$ and I are XAS intensities measured with $\mathbf{E} \perp c$ and with $\mathbf{E}$ in the plane defined by the c axis and the direction of incident radiation, respectively.
[25] W. B. Wu *et al.* (to be published).
[26] We used $10Dq = 2.2$ eV, $\Delta_i = 0.1$ eV, and $\Delta_f = 0.5$ eV. Other parameters are the same as those in Ref. [21].
[27] J. van Elp and A. Tanaka, Phys. Rev. B **60**, 5331 (1999).
[28] We used $U = 8.0$ eV, $10Dq = 2.0$ eV, charge-transfer energy $\Delta = 2.1$ eV, and $pd\sigma = 2.1$ eV.
[29] G. Y. Guo *et al.* (unpublished).
[30] S. Larochelle *et al.*, Phys. Rev. Lett. **87**, 095502 (2001).
[31] The longer and shorter in-plane Mn-O lengths are, respectively, 2.00 and 1.84 Å, while the out-of-plane Mn-O length is 1.98 Å.
[32] P. G. Radaelli *et al.*, Phys. Rev. B **55**, 3015 (1997).
[33] Y. Konishi *et al.*, J. Phys. Soc. Jpn. **68**, 3790 (1999).
[34] Z. Fang, I. V. Solovyev, and K. Terakura, Phys. Rev. Lett. **84**, 3169 (2000).
[35] C. W. M. Castleton and M. Altarelli, Phys. Rev. B **62**, 1033 (2000).